Acta Ciencia Indica, Vol. XLIII C, No. 2, 135 (2017)

COMPUTATIONAL STUDIES ON PYRAZOLONES AS KDR INHIBITORS

DR. POOJA SAPRA
C.S.S.S (P.G.) College, Machhra, Meerut

RECEIVED : 13 April, 2017

Pyrazolone is a five membered lactum ring containing two nitrogens and a ketone group in its ring and are the oldest synthetic pharmaceuticals alongwith aspirin and acetaminophen. When pyrazolones were first discovered, they were only known as non-steroidal anti-inflammatory drug (NSAID) but in recent times, they are known to exhibit antioxidant, anticancer, antibacterial and several other pharmacological actions. KDR/VEGFR-2 (Vascular endothelial growth factor receptor) a tyrosine kinase, is considered to play a pivotal role in angiogenesis, the process involving formation of new capillaries from pre-existing blood vessels. Taking in account the inhibitory activities of pyrazolone against KDR and importance of computational study, it was considered worthwhile to perform semi-empirical calculations and binding studies on these molecules. This study provide explanation to the variation in the biological activities of the pyrazolone derivatives using charge densities, HOMO-LUMO energies and through binding data.

KEYWORDS : KDR, angiogenesis, pyrazolones, computational chemistry.

INTRODUCTION

The chemistry of pyrazolone began in 1883 when Knorr reported the first pyrazolone derivative. Knorr pyrazole synthesis is the reaction of hydrazines with 1, 3-dicarbonyl compounds to provide the pyrazole or pyrazolone ring system. The reaction of phenyl hydrazine and ethylacetoacetate resulted in novel structure identified in 1887 as 1-phenyl-3-methyl-5-pyrazolone [1]. Pyrazolones are best classified as follows: 5-pyrazolone **1**, also called 2-pyrazolin-5-one, 4-pyrazolone **2**, also called 2-pyrazolin-4-one; and 3-pyrazolone **3**, also called 3-pyrazolin-5-one. Within each class of pyrazolones many tautomeric forms are possible [2].

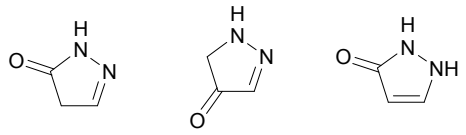

(**1**) (**2**) (**3**)

Fig. 1: Pyrazolones

When pyrazolones were first discovered, they were only known as non-steroidal anti-inflammatory drug (NSAID, Antipyrine **4** and Aminophenazone or Aminopyrine **5**) but in recent times, they are known to exhibit antioxidant [3], anticancer [4], antibacterial [5] and several other pharmacological actions [6].

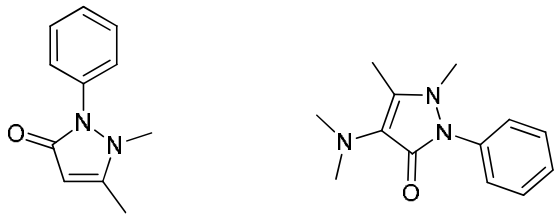

(**4**) (**5**)

Fig. 2. Pyrazolones based NSAIDs

Kinases have attracted a lot of attention, as many diseases such as various cancers; autoimmune diseases etc have been associated with deregulated activity of kinases [7, 8]. The successful proof of concept has resulted in launching of many kinase inhibitors as drugs against cancer, RA (examples such as imatinib, ibrutinib, trametinib, palbociclib), etc. Many more kinase inhibitors are in clinical pipelines. VEGFR-2 (Vascular endothelial growth factor receptor, also known as KDR) a tyrosine kinase, is considered to play a pivotal role in angiogenesis, the process involving formation of new capillaries from pre-existing blood vessels [9]. Tumor angiogenesis is a prerequisite for tumor growth as it is a fundamental step in the transition of tumors from a dormant state to a malignant one [10]. Inhibition of tumor angiogenesis is a novel technique to stop the tumor growth, which eventually can be destroyed. The successful launch of VEGFR-2 inhibitors such as pazopanib, sorafenib, ponatinib, regorafenib, etc has proven the importance of such molecules. Computer based drug design has played an important part in designing of small molecule inhibitors against various targets especially in case of kinase inhibitors. Computational studies have helped researchers and pharmaceutical company to make prediction of activity of a small molecule inhibitor in a cost effective and environmental friendly manner [11].

Object of Present Work

Taking in account of the inhibitory activities of pyrazolone against KDR and importance of computational study, it was considered worthwhile to perform semi-empirical calculations and binding studies on these molecules. This study attempts to provide explanation to the variation in the biological activities of the pyrazolone derivatives using charge densities, HOMO-LUMO energies and through binding data.

MATERIALS AND METHODS

The structures of the molecules (Figure 3a, 4a) under study were constructed using ISIS Draw software (version 2.4). The geometries were subsequently optimized (Figure 3b, 4b) and partial atomic charges and HOMO, LUMO energies (Table 1, 2) were calculated using semi-empirical program MOPAC 2009 [12] package applying RM1 Hamiltonian in gas phase. The binding studies were carried out using AUTODOCK 4.0 (http://autodock.scripps.edu/) [13]. The file used for KDR kinase (1 YWN) was downloaded from protein data bank (PDB) (www.pdb.org).

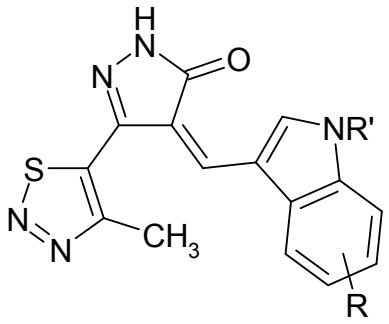

Fig. 3a: Substituted Pyrazolone (1)

Table 1. KDR Inhibitory Activities and RM1 Calculated Values for Various Substituted Pyrazolone (1) [14].

Compd No.	R	R'	Charge density on N in Pyrazolone	Charge density on N of NH in Pyrazolone	Charge density on O of C=O in Pyrazolone	HOMO Energies (eV)	LUMO Energies (eV)	Energy differnce (HOMO-LUMO) (eV)	IC_{50} Value (nM)
1	H	H	-0.1087	-0.3401	-0.3957	-8.556	-1.045	-7.511	>1000
1 (a)	H	CH_3	-0.1108	-0.3403	-0.3987	-8.442	-0.997	-7.445	95
1 (b)	5-F	CH_3	-0.1095	-0.3389	-0.3988	8.616	-1.105	-7.511	99
1 (c)	5-Cl	CH_3	-0.1077	-0.3394	-0.3965	-8.647	-1.139	-7.508	152
1 (d)	5-Cl	H	-0.1065	-0.3391	-0.3959	-8.764	-1.189	-7.575	>300
1 (e)	5-OCH_3	CH_3	-0.1139	-0.3397	-0.4033	-8.339	-0.95	-7.389	90
1 (f)	5-CN	CH_3	-0.105	-0.3387	-0.3938	-8.781	-1.271	-7.51	>300
1 (g)	4-F	CH_3	-0.1101	-0.3395	-0.3976	-8.528	-1.064	-7.464	137
1 (h)	4-Cl	CH_3	-0.1124	-0.3388	-0.3987	-8.567	-1.066	-7.501	45
1 (i)	4-Br	CH_3	-0.1128	-0.3386	-0.4004	-8.561	-1.048	-7.513	34
1 (j)	4-OCH_3	CH_3	-0.1143	-0.3398	-0.3995	-8.25	-1.938	-6.312	19
1 (k)	4-OC_2H_5	CH_3	-0.1157	-0.339	-0.4000	-8.23	-1.941	-6.289	38
1 (l)	4-CH3	CH_3	-0.1126	-0.3386	-0.3997	-8.355	-1.012	-7.343	58
1 (m)	4-Br, 5-OCH_3	CH_3	-0.1159	-0.3381	-0.4051	-8.43	-1.973	-6.487	23
1 (n)	7-OCH_3	CH_3	-0.1126	-0.3403	-0.4002	-8.28	-0.939	-7.341	109
1 (p)	4-OCH_3, 7- OCH_3	CH_3	-0.1156	-0.3399	-0.4005	-8.08	-0.896	-7.184	20

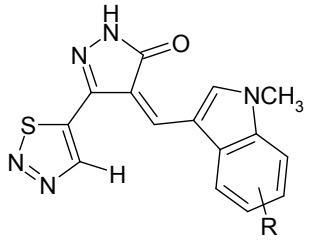

Fig. 4a: Substituted Pyrazolone (2)

Table 2. KDR Inhibitory Activities and RM1 Calculated Values for Various Substituted Pyrazolone (2) [14].

Compd No.	R	Charge density on N in Pyrazolone	Charge density on N of NH in Pyrazolone	Charge density on O of C=O in Pyrazolone	HOMO Energies (eV)	LUMO Energies (eV)	Energy differnce (HOMO-LUMO) (eV)	IC_{50} Value (nM)
2 (a)	5-F	-0.1082	-0.3358	-0.3964	-8.637	-1.203	-7.434	48
2 (b)	5-Cl	-0.1069	-0.3358	-0.3941	-8.668	-1.243	-7.425	34
2 (c)	5-CN	-0.1039	-0.3354	-0.3914	-8.802	-1.353	-7.449	174
2 (d)	5-$COOCH_3$	-0.1051	-0.3361	-0.3913	-8.693	-1.293	-7.4	73
2 (e)	5-OCH_3	-0.1112	-0.3362	-0.3984	-8.448	-1.112	-7.336	28
2 (f)	5-Br	-0.1069	-0.3360	-0.3939	-8.653	-1.233	-7.42	110
2 (g)	5-CH_3	-0.1111	-0.3366	-0.3973	-8.424	-1.096	-7.328	35
2 (h)	4-F	-0.1091	-0.3363	-0.3953	-8.549	-1.161	-7.388	16
2 (i)	4-Cl	-0.1106	-0.3360	-0.3976	-8.579	-1.142	-7.437	16
2 (j)	4-Br	-0.1110	-0.3360	-0.3982	-8.579	-1.131	-7.448	8
2 (k)	4-OCH_3	-0.1126	-0.3372	-0.3972	-8.264	-1.033	-7.231	13
2 (l)	4-OC_2H_5	-0.1143	-0.3362	-0.3976	-8.242	-1.043	-7.199	25
2 (m)	4-$COOCH_3$	-0.0976	-0.3473	-0.3616	-8.660	-0.998	-7.662	22
2 (n)	4-Br, 5-OCH_3	-0.1140	-0.3354	-0.4020	-8.471	-1.075	-7.396	6
2 (o)	6-Cl	-0.1063	-0.3356	-0.3931	-8.654	-1.263	-7.391	73
2 (p)	4-Br, 6-CH_3	-0.1115	-0.3362	-0.3977	-8.524	-1.112	-7.412	12
2 (q)	4-OCH_3,7-OCH_3	-0.1139	-0.3372	-0.3984	-8.084	-0.991	-7.093	10

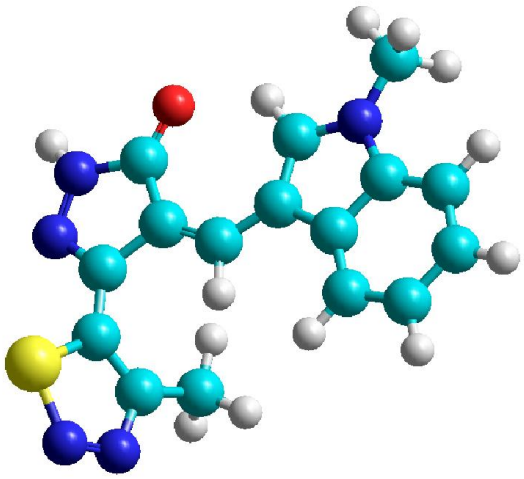

Fig. 3b: Optimizied geometry of 1(a) (Blue = Nitrogen, Red = Oxygen, Yellow = Sulphur)

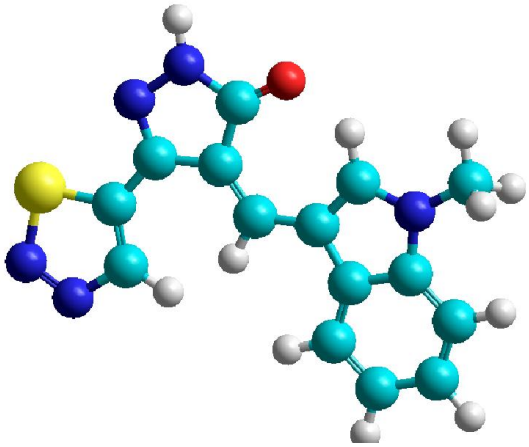

Fig. 4b: Optimizied geometry of 2 (Blue = Nitrogen, Red = Oxygen, Yellow = Sulphur)

RESULTS AND DISCUSSION

1, 2, 3-Thiadiazole substituted Pyrazolones are reported as potent KDR inhibitors. The possible binding modes of the pyrazolones with KDR are represented in Figure 5 [14, 15].

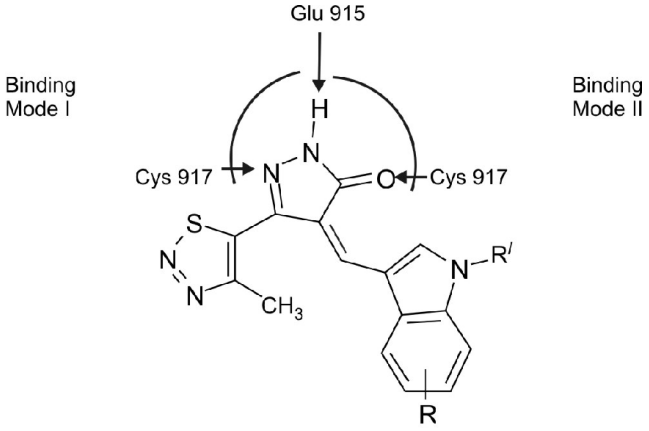

Fig. 5: Predicted binding modes of pyrazolones with KDR.

Recent studies on this scaffold have provided the researchers with few interesting findings for an optimal KDR-inhibitor binding [14]. It is proposed that the activity of the 1,2,3-Thiadiazole substituted pyrazolones depends upon following structural parameters:

1. The N, NH, and the carbonyl group of the pyrazolone will play a role in the backbond hydrogen bond. Though the combination of NH and CO is preferred as backbond hydrogen, but the acceptor N too can play a part in binding (Figure 5).
2. The restricted rotation offered by the exocyclic double bond to the lactam unit plays a significiant role in binding.
3. N-Methyl substitution on the indole ring is preferred.

4. The configuration of the double bond was determined to be 'Z' on the basis of ^{1}H NMR observations. The indole proton at 2-position showed a significant downfield shift being proximal to the lactam carbonyl in a Z configuration [15].

Molecular modelling results based on the Glide XP docking approach have supported the postulation regarding interaction of the lactam segment of the pyrazolones with the hinge region of the KDR kinase. The lactam ring of the pyrazolone has one hydrogen donor NH flanked by two hydrogen acceptors, that is, the carbonyl O and N. This may lead to two possible binding modes of the pyrazolone ring in the hinge region: either the hydrogen acceptor O or the N may bind with the Cys-917 backbone NH (Figure 5) [14].

The potency of the inhibitor depends directly upon the strength of its binding with the KDR. Ligand-receptor binding is optimal when the number of favourable interactions overweighs their unfavourable interactions. In case of pyrazolone-KDR binding, the favourable contacts consist of hydrogen bonding and hydrophobic-hydrophobic interactions, whereas unfavourable contacts consist of hydrophobic-polar interactions. In addition to the above stated hydrogen bonds, interactions of a thiadiazole/indole with aliphatic residues of KDR (hydrophobic-hydrophobic) and of the 4th substituent with hydrophobic ATP-pocket of KDR to play a very important role. Moreover, the most frequently occurring binding mode had the pyrazolone C=O bound to the Cys-917 NH and the thiadiazole ring near the salt bridge Lys-866.

Keeping in mind that combination of above four parameters are responsible for the potency of this family against KDR; a suitable set of inhibitor molecules was selected for the study. The results of the semi-empirical calculations on the selected substituted pyrazolones carried out using AM1 subroutine using MOPAC 2009[12] showed pyrazolone nitrogen with unexpected positive charge densities, to overcome this anomalous behaviour, the calculations were done using RM1 subroutine. The results of calculations are reported in Table 1 and 2.

A qualitative comparison of various pyrazolones suggests that potency can be correlated with the energy gap between HOMO-LUMO energies. A lower modulus of the value for HOMO-LUMO energy is reciprocated with a higher potency value, suggesting that a good electron donor character of pyrazolones is required for an efficient binding with KDR in its binding cleft. Molecule 1(m) and 1(j) from Table 1 (IC_{50} = 23, 19 nM) are two best suited examples showing an energy difference of -6.487 and -6.312 eV respectively. On comparing energy levels of lesser potent molecules such as 1(a), 1(b) (IC_{50} = 95, 99 nM), the energy gap rises to -7.445, -7.511 eV respectively. This rise suggests a poor capacity on the part of the molecule to part with charge during the binding process in the KDR binding cleft. Such a failure will result in lesser number of favourable ligand-KDR interactions, resulting in poor binding and a lower value of inhibition (as well potency) of the inhibitor. The electron charges on the carbonyl oxygen too suggest its possible role-play in effective backbone hydrogen bonding, which then determine the level of potency in the molecules. The potent molecules of the series, 1(j) and 1(m) have charge density of -8.25 and -8.43 eV respectively, where the least potent one such as 1(a) and 1(b) have the values -8.442 eV and -8.616 eV, favoring a more directed hydrogen bond in case 1(j) and 1(m). A higher electron charge density in carbonyl carbon is complimented with a lower charge density on pyrazolone N in most of the molecules. This might suggest the shift of the bonding preference for backbone hydrogen bond in series, with a relative preference for N of pyrazolone or O of the carbonyl.

An attempt was made to understand structure activity relationship of inhibitor's potency with respect to the substitution in the 4th and 5th position of the indole ring. In general the substitution on the 4th position provided molecules with better potency than those at position 5th. The HOMO-LUMO energy gap for molecules 1(c), and 1(h) are -7.508 and -7.501

respectively but have significant different IC_{50} values (152, 45 nM, respectively). This suggests that the restricted rotation offered by the bulky 5th subsitutent to the indole ring has resulted in the loss of the potency. These finding concur with CoMFA and CoMSIA model that suggest a positive bulk with hydrophobic effect is desirable around 4th, 5th position and hydrogen bond acceptor groups around pyrazolones ring will be helpful [16]. The charge density on N of pyrazolone and O of carbonyl are reversed in these two molecules, suggesting a possibility of involvement of NH and CO in backbone hydrogen bond for 1(h) and N and NH in case of 1(c).

The nature of the substituent too plays a role in the binding behaviour of the inhibitors in the binding cleft. Highly electronegative substituent like fluoro, cyano etc, have higher HOMO-LUMO energy gap, as compared to electron donating substituents like methoxy, ethoxy etc. This supports the observation that for a tighter binding (and a good potency) the pyrazolone molecules should be electron rich, so that they can have effective interaction in the KDR binding cleft.

In second series of pyrazolone derivatives, the methyl group in thiadiazole ring is substituted with a hydrogen atom. The potency and its relation to HOMO-LUMO energy gap remain same as that for series 1. The molecule with same substitution showed better potency in series 2 as compared to series 1, even a less potent molecule like 1(c) (IC_{50} = 152 nM) displayed a better value 2(b) (IC_{50} = 34 nM) in series 2. This substitution with hydrogen provides better rotatory movement for the thiadiazole ring in the KDR binding cleft, allowing it to take better orientations for a perfect binding. This freedom of rotation provided molecules with better potency than those in series 1. Thus Bulky group are easily accommodated by the indole ring in series 2, providing with more options to understand structure activity relationship.

These semi-empirical calculation results were further cemented by the results of the binding studies on pyrazolones with KDR done using Autodock 4.0. These results strengthen the observations regarding the interaction of the lactam ring of the pyrazolone in the hinge region of KDR, as can be seen in Figure 5. The sailent features of the docking studies are-

1. The most frequently occurring binding mode was one where the oxygen of pyrazolone was close to Cys-917 NH and the nitrogen was bonded to the Glu 915. These interactions are expected to be the backbone hydrogen bonds.
2. The most stable binding had thiadiazole ring near the salt bridge Lys-866.

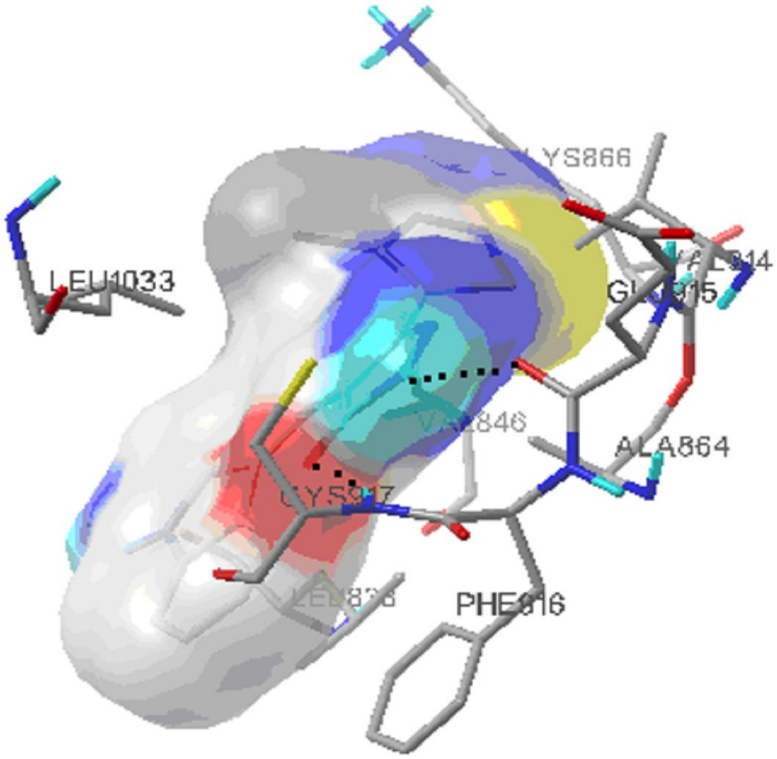

Fig. 6: Favourable binding mode of KDR with compound (1). The dotted lines show hydrogen bonds.

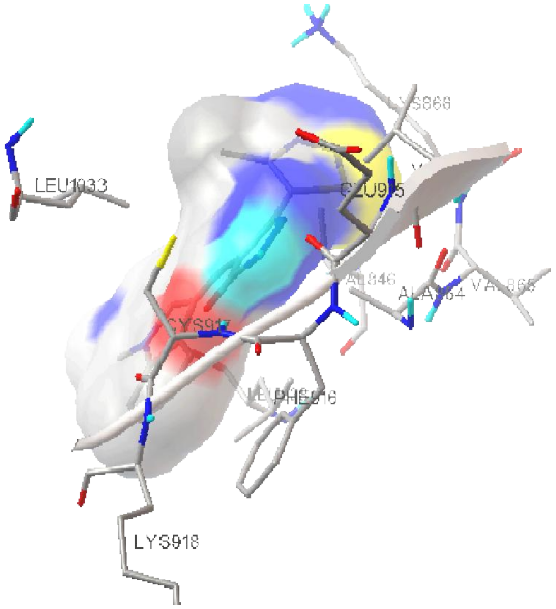

Fig. 7. Favourable binding mode of KDR with compound (1a). The dotted lines show hydrogen bonds.

Both the binding pattern did not have a significant energy difference between them, so as to decisively favour one structure over the other. The **figure 6** and **7** shows binding of **1** and **1(a)** in the KDR binding cleft. The backbone hydrogen bond involved CO of the pyrazolone with NH of Cys-917 and CO of Glu-915 with NH of pyrazolone. The thiadiazole ring is closer to Lys-866. In few cases the postulated second mode of binding involving nitrogen and NH of the pyrazolone was also seen. No clear SAR correlation could be carried out, but in these configurations the thiadiazole ring was placed far away from the salt bridge Lys-866.

One interesting finding of the binding study was a possible explanation for the good potency value of **2(q)** and **1(p)** as compared to their respective series members. In **1(p)** and **2(q)** one extra hydrogen bond involving ASN-921 of KDR and methoxy group at 7th position of the indole ring was observed apart from backbone hydrogen bonds. This hydrogen bond involving ASN-921 could be the possible reason for good potency shown by **1(p)** (IC_{50} = 20 nM) and **2(q)** (IC_{50} = 10 nM) respectively.

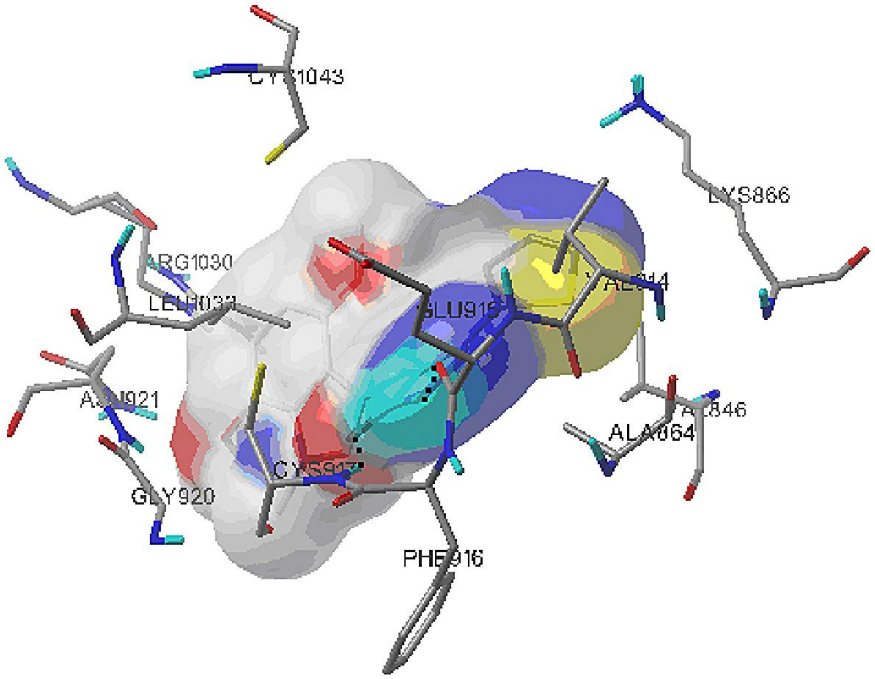

Fig. 8: Favourable binding mode of KDR with compound (1p). The dotted lines show hydrogen bonds.

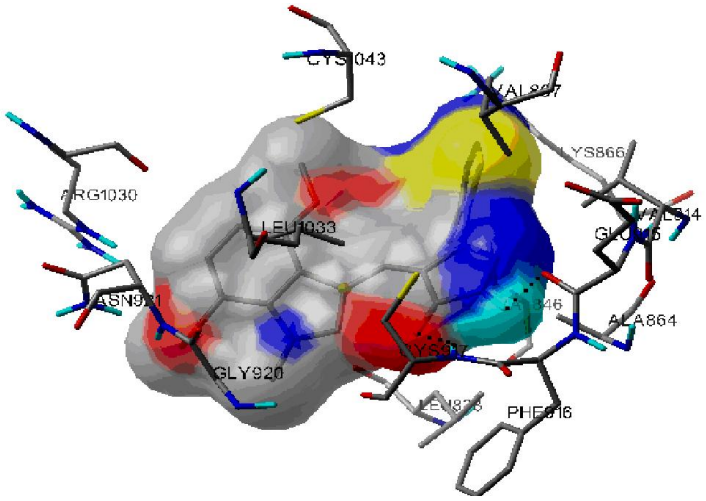

Fig. 9: Favourable binding mode of KDR with compound (2q). The dotted lines show hydrogen bonds.

Molecule **2(n)** like most member of the series showed both the preferred mode of binding. Both of the modes are represented in **figure 10** and **11**. In case of the first binding mode (Figure 10), apart from the backbone hydrogen bond involving, NH and CO of pyarazolone with Glu-915 and Cys-917, respectively. The 2.2 Å distance between ASN-921 and oxygen of methoxy group suggest the presence of an extra hydrogen bond. The second binding mode is deprived of this interaction suggesting that first mode is favoured in this case. This new hydrogen bonding involving ASN-921 should be responsible for its high potency (IC_{50} = 6 nM).

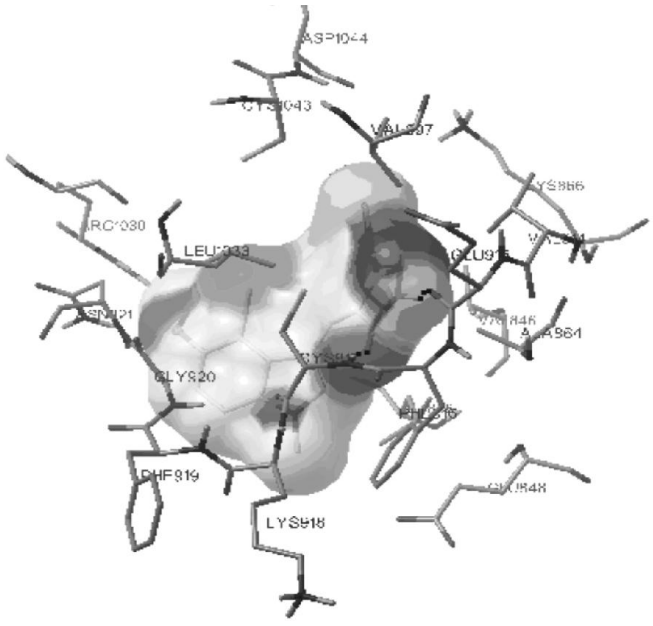

Fig. 10. Favourable binding mode of KDR with compound (2n). The dotted lines show hydrogen bonds.

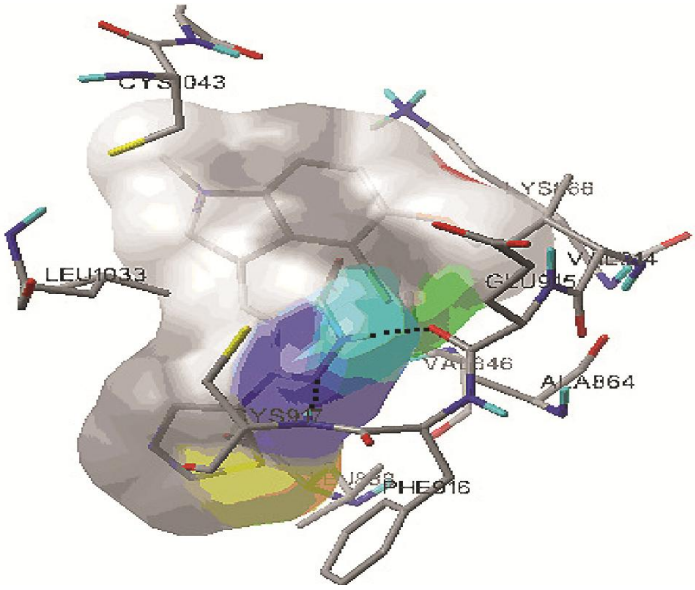

Fig. 11: Unfavourable binding mode of KDR with compound (2n). The dotted lines show hydrogen bonds.

Conclusions

A lower value of the HOMO-LUMO energy difference is reciprocated with a higher potency value, suggesting that a good electron donor character of pyrazolones is required for an efficient binding with KDR in its binding cleft. A higher electron charge density in carbonyl carbon is complimented with a lower charge density on pyrazolone N in most of the molecules. This might suggest the shift of the bonding preference for backbone hydrogen bond in series, with a relative preference for N of pyrazolone or O of the carbonyl. In general the substitution on the 4th position of indole provided molecules with better potency than those at position 5th possibly due to restricted rotation offered by bulky group at position 5th. Further potency also depends on the number of hydrogen bonds. Inhibitor molecules with extra hydrogen bonds other than the backbone hydrogen bonds are more potent. These observations can help synthetic chemist to design new selective inhibitors of KDR with better potency.

References

1. Li, J. J., Knorr Pyrazole Synthesis, *Springer,* Berlin Heidelberg New York, 331-334 (2006).
2. Pyrazoles, Pyrazolines and Pyrazolones, *Kirk-Othmer Encyclopedia of Chemical Technology*. 4th Eds. John Wiley & Sons, Inc. (1998).
3. Idemudia, O. G., Sadimenko, A. P. and Hosten, E. C., *Int. J. Mol. Sci.*, **17**, 687 (2016).
4. Ghorab, M. M., El-Gazzar, M. G. and Alsaid, M. S., *Int. J. Mol. Sci.*, **15**, 7539 (2014).
5. Alam, M. S. and Lee, D. U., *EXCLI J*, **16**, 614 (2016).
6. Mariappan, G., Saha, B. P., Sutharson, L., Ankits, G., Pandey, L. and Kumar, D., *J. Pharm Res.*, **3**, 2856 (2010).
7. Singh, V., Ram, M., Kumar, R., Prasad, R., Roy, B. K. and Singh, K. K., *Protein, J.*, **36**, 1 (2017).
8. Pernis, A. B., Ricker, E., Weng, C. H., Rozo, C. and Yi, W., *Annu Rev Med*, **67**, 355 (2016).
9. Sharma, P. S., Sharma, R. and Tyagi, T., *Curr Cancer Drug Targets*, **11**, 624 (2011).
10. Folkman, J., Role of angiogenesis in tumor growth and metastasis, *Semin Oncol*, **29**, 15 (2002).
11. Carmer, C. J., *Essential of computational chemistry,* **2nd Edition**, John Wiley Publication (2004).
12. Stewart, J. J. P., MOPAC, Program Package, Academic free copy (2009).

13. Goodsell, D. S., Morris, G. M. and Olson, A. J., *J. Mol. Recognit*, **9**, 1 (1996).
14. Tripathy, R., Ghose, A., Singh, J., Bacon, E. R., Angeles, T. S., Yang, S. X., Albom, M. S., Aimone, L. D., Herman, J. L. and Mallamo, J. P., *Bioorg Med Chem Lett*, **17,** 1793 (2007).
15. Tripathy, R., Reiboldt, A., Messina, P. A., Iqbal, M., Singh, J., Bacon, E. R., Angeles, T. S., Yang, S. X., Albom, M. S., Robinson, C., Chang, H., Ruggeri, B. A, and Mallomo, J. P., *Bioorg Med Chem Lett*, **16**, 2158 (20006).
16. Pasha, F. A., Muddassar, M., Neaz, M. M. and Cho, S J., *J. Mol. Graph Model*, **28**, 54 (2009).

❑